

Homogeneous electrochemical water oxidation catalyzed by cobalt complexes with amine-pyridine ligand

Yanmei Chen^{a*}, Xiangyu Meng^b, Xiaoli Chen^a, Xinyi Li^a, Hui Ye^a, Shanshan Liu^a, Zhijun Ruan^a, Xiangming Liang^{c*}, Junqi Lin^{a*}

^a Hubei Key Laboratory of Processing and Application of Catalytic Materials, College of Chemistry and Chemical Engineering, Huanggang Normal University, Huanggang, 438000 China. Email: cingym@163.com, linjunqi@hgnu.edu.cn.

^b Henan Provincial Key Laboratory of Nanocomposites and Applications, Institute of Nanostructured Functional Materials, Huanghe Science and Technology College, 666 Zijing Mountain South Road, Zhengzhou, Henan 450006, China.

^c School of Basic Medical Sciences, Ningxia Medical University, Yinchuan 750004, China.
Email: liangxm6@163.com

Table S1 Crystallographic data and processing parameters of complex **1**

Complex parameters	Complex 1
Empirical formula	C ₂₁ H ₂₅ N ₅ Cl ₂ O ₈ Co
Formula weight	605.29
Temperature / K	280.0
Wavelength / Å	0.71073
Crystal system	Monoclinic
Space group	Cc
<i>a</i> / Å	13.9770(12)
<i>b</i> / Å	10.8038(10)
<i>c</i> / Å	16.1388(16)
α / deg	90
β / deg	93.597(3)
γ / deg	90
Volume / Å ³	2529.94(40)
<i>Z</i>	4
Calculated density / Mg m ³	1.58905
Absorption coefficient / mm ⁻¹	0.946
<i>F</i> (000)	1244
Crystal size / mm ³	0.320 × 0.260 × 0.310
θ range / deg	2.60 to 25.01
	-18 ≤ <i>h</i> ≤ 18
Index ranges	-14 ≤ <i>h</i> ≤ 14
	-20 ≤ <i>h</i> ≤ 20
Reflections collected	27821
Independent reflections	5777 [<i>R</i> (int) = 0.0607]
Completeness to theta	99.5% (25.01°)
Refinement method	Full-matrix least-squares on <i>F</i> ²
Data / restraints / parameters	5777 / 2 / 336
Goodness-of-fit on <i>F</i> ²	1.028
Final <i>R</i> indices [<i>I</i> > 2σ(<i>I</i>)]	<i>R</i> ₁ = 0.0669, <i>wR</i> ₂ = 0.0951
<i>R</i> indices (all data)	<i>R</i> ₁ = 0.0406, <i>wR</i> ₂ = 0.1072
Largest diff. peak and hole	0.354 and -0.384 e.Å ⁻³

$$R_1 = \Sigma||F_o| - |F_c||/\Sigma|F_o|, wR_2 = [\Sigma(|F_o|^2 - |F_c|^2)^2/\Sigma(F_o2)]^{1/2}$$

Table S2 Crystallographic data and processing parameters of complex **2** and [Zn(N3Py2)(OH2)](ClO4)2

Complex parameters	Complex 2	[Zn(N3Py2)(OH2)](ClO4)2
Empirical formula	C ₁₉ H ₃₁ N ₅ Cl ₂ O ₉ Co	C ₁₉ H ₃₁ N ₅ Cl ₂ O ₉ Zn
Formula weight	603.32	609.76
Temperature / K	273.2	273.0
Wavelength / Å	0.71073	0.71073
Crystal system	Monoclinic	Monoclinic
Space group	<i>P</i> 2 ₁ / <i>c</i>	<i>P</i> 2 ₁ / <i>c</i>
<i>a</i> / Å	9.0629 (18)	9.0470(13)
<i>b</i> / Å	33.221 (8)	33.224(4)
<i>c</i> / Å	8.842 (2)	8.7975(14)
α / deg	90	90
β / deg	104.732 (9)	104.960(5)
γ / deg	90	90
Volume / Å ³	2574.6 (11)	2554.7(6)
<i>Z</i>	4	4
Calculated density / Mg m ³	1.557	1.585
Absorption coefficient / mm ⁻¹	0.931	1.228
<i>F</i> (000)	1252	1264
Crystal size / mm ³	0.220 × 0.210 × 0.170	0.270 × 0.290 × 0.260
θ range / deg	2.60 to 25.01	2.33 to 26.38
	-11 ≤ <i>h</i> ≤ 11	-11 ≤ <i>h</i> ≤ 11
Index ranges	-43 ≤ <i>h</i> ≤ 43	-41 ≤ <i>h</i> ≤ 41
	-11 ≤ <i>h</i> ≤ 11	-11 ≤ <i>h</i> ≤ 11
Reflections collected	29858	61767
Independent reflections	5876 [<i>R</i> (int) = 0.0638]	5215 [<i>R</i> (int) = 0.0607]
Completeness to theta	99.5% (25.01°)	99.7% (25.01°)
Refinement method	Full-matrix least-squares on <i>F</i> ²	
Data / restraints / parameters	5876 / 0 / 329	5215 / 0 / 329
Goodness-of-fit on <i>F</i> ²	1.028	1.036
Final <i>R</i> indices [<i>I</i> > 2σ(<i>I</i>)]	<i>R</i> ₁ = 0.0949, <i>wR</i> ₂ = 0.1778	<i>R</i> ₁ = 0.0827, <i>wR</i> ₂ = 0.1574
<i>R</i> indices (all data)	<i>R</i> ₁ = 0.0638, <i>wR</i> ₂ = 0.2034	<i>R</i> ₁ = 0.0586, <i>wR</i> ₂ = 0.1777
Largest diff. peak and hole	1.347 and -0.640 e.Å ⁻³	1.628 and -0.771 e.Å ⁻³

$$R_1 = \sum ||F_o| - |F_c|| / \sum |F_o|, wR_2 = [\sum (|F_o|^2 - |F_c|^2)^2 / \sum (F_o^2)]^{1/2}$$

Table S3 Selected bond lengths (Å) and angles (deg) of **1**

Complex	1
Bond length (Å)	
Co1–N1	2.046(10)
Co1–N2	2.051(9)
Co1–N3	2.174(8)
Co1–N4	2.184(8)
Co1–N5	2.024(3)
Bond angles (deg)	
N1–Co1–N2	101.60(13)
N1–Co1–N3	79.34(34)
N1–Co1–N4	115.95(34)
N1–Co1–N5	128.73(28)
N2–Co1–N3	115.44(34)
N2–Co1–N4	80.20(34)
N2–Co1–N5	129.64(25)
N3–Co1–N4	156.63(32)
N3–Co1–N5	77.31(32)
N4–Co1–N5	79.32(32)

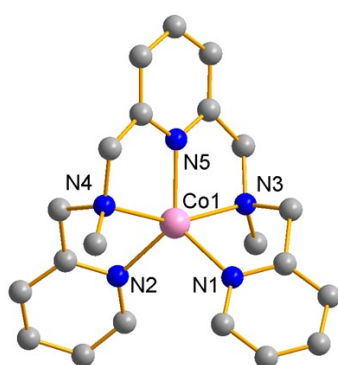
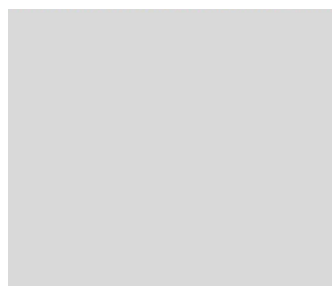
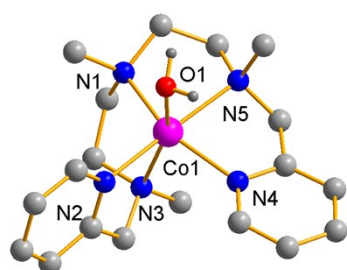
**Fig. S1** The atom label of cations of complex **1**.

Table S4 Selected bond lengths (Å) and angles (deg) of **2** and [Zn(N3Py2)(OH₂)](ClO₄)₂

Complex	2	Complex	[Zn(N3Py2)(OH ₂)](ClO ₄) ₂
Bond length (Å)		Bond length (Å)	
Co1–N1	2.157(3)	Zn1–N1	2.188(4)
Co1–N2	2.165(4)	Zn1–N2	2.132(4)
Co1–N3	2.245(5)	Zn1–N3	2.256(4)
Co1–N4	2.142(3)	Zn1–N4	2.262(3)
Co1–N5	2.233(4)	Zn1–N5	2.155(4)
Co1–O1	2.146(3)	Zn1–O1	2.175(3)
Bond angles (deg)		Bond angles (deg)	
N1–Co1–N2	103.90(14)	N1–Zn1–N2	99.39(14)
N1–Co1–N3	81.71(15)	N1–Zn1–N3	76.03(14)
N1–Co1–N4	153.98(15)	N1–Zn1–N4	127.44(13)
N1–Co1–N5	80.92(14)	N1–Zn1–N5	104.10(15)
N1–Co1–O1	96.34(15)	N1–Zn1–O1	84.13(13)
N2–Co1–N3	75.86(13)	N2–Zn1–N3	94.40(16)
N2–Co1–N4	99.38(13)	N2–Zn1–N4	76.64(14)
N2–Co1–N5	173.43(14)	N2–Zn1–N5	154.61(15)
N2–Co1–O1	85.44(13)	N2–Zn1–O1	95.96(14)
N3–Co1–N4	92.99(14)	N3–Zn1–N4	110.48(14)
N3–Co1–N5	109.54(13)	N3–Zn1–N5	82.19(16)
N3–Co1–O1	160.04(13)	N3–Zn1–O1	158.87(14)
N4–Co1–N5	76.91(13)	N4–Zn1–N5	81.02(14)
N4–Co1–O1	96.94(13)	N4–Zn1–O1	89.84(13)
N5–Co1–O1	89.61(13)	N5–Zn1–O1	95.88(16)

**Fig. S2** The atom label of cations of complex **2** (left) and [Zn(N3Py2)(OH₂)](ClO₄)₂ (right).

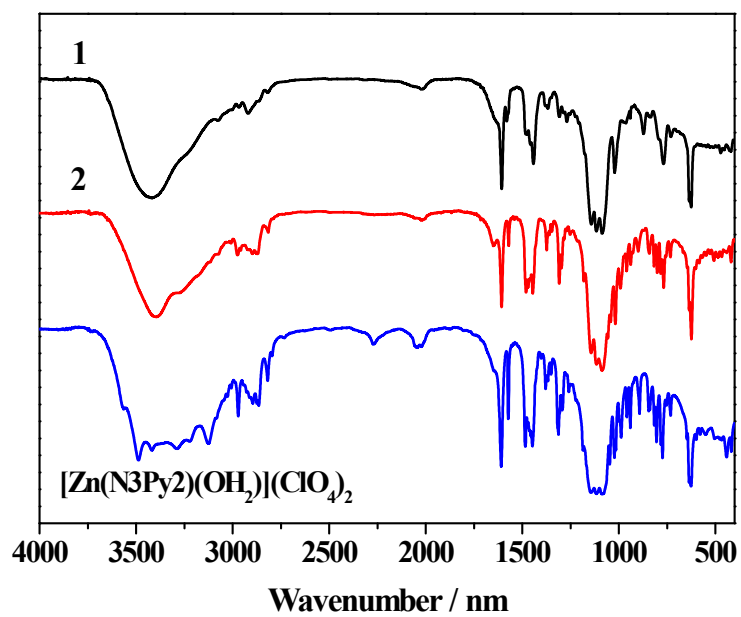


Fig. S3 Infrared spectra of complex 1, 2, and $[\text{Zn}(\text{N3Py2})(\text{OH}_2)](\text{ClO}_4)_2$.

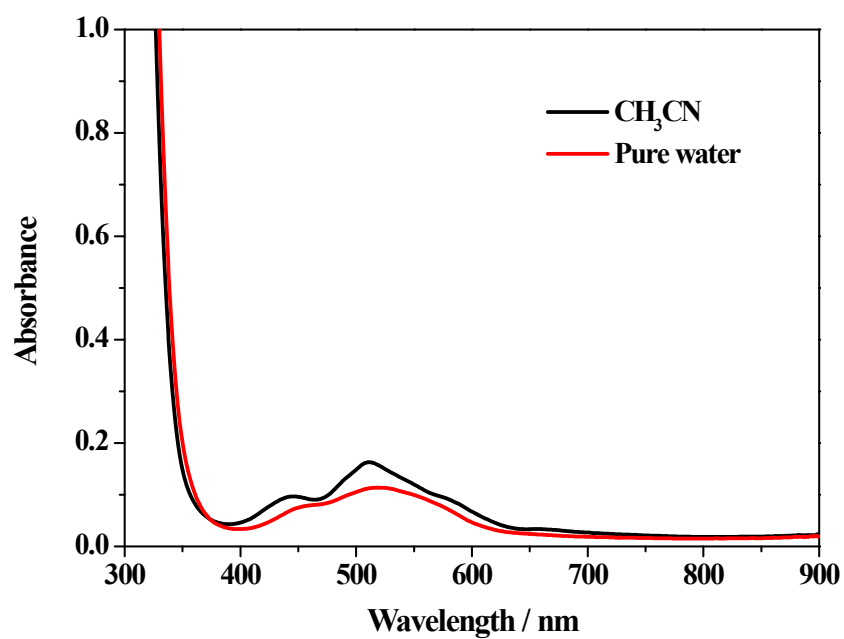


Fig. S4 UV-vis absorption spectra of 5 mM of complex 1 in CH_3CN and pure water.

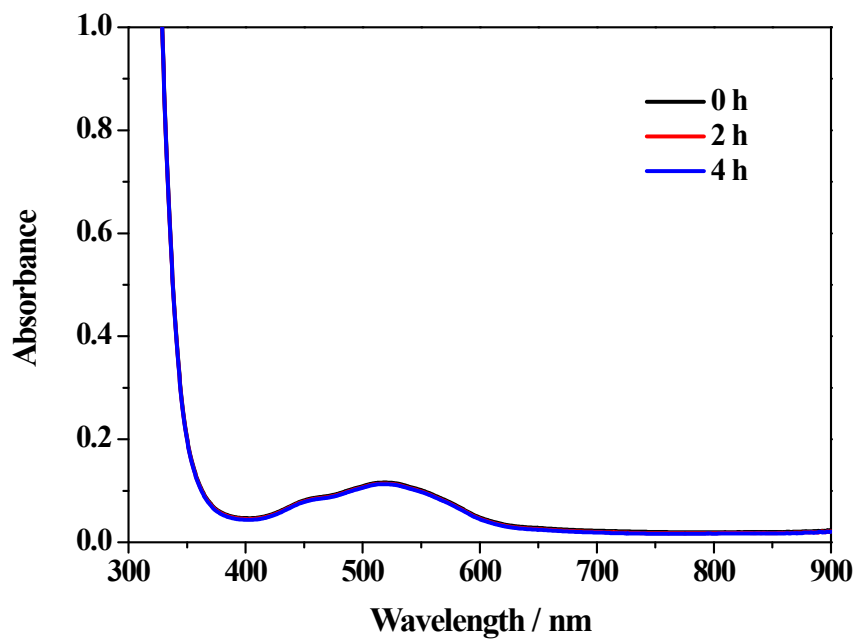


Fig. S5 UV-vis absorption spectra of 5 mM of complex **1** with different aging time in PBS at pH 3.0.

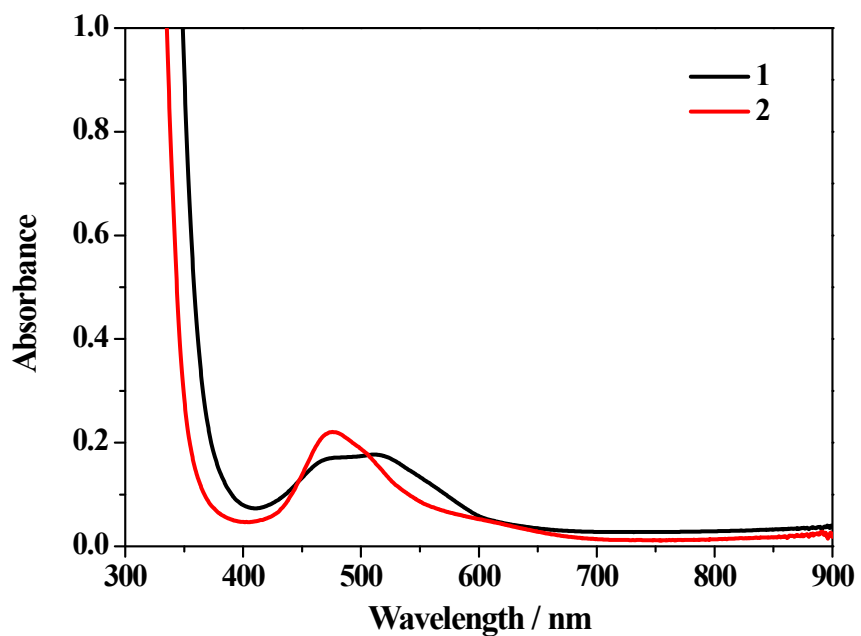


Fig. S6 UV-visible absorption spectra of complex **1** and **2** in 0.1 M phosphate buffer solution (PBS) at pH 11.0.

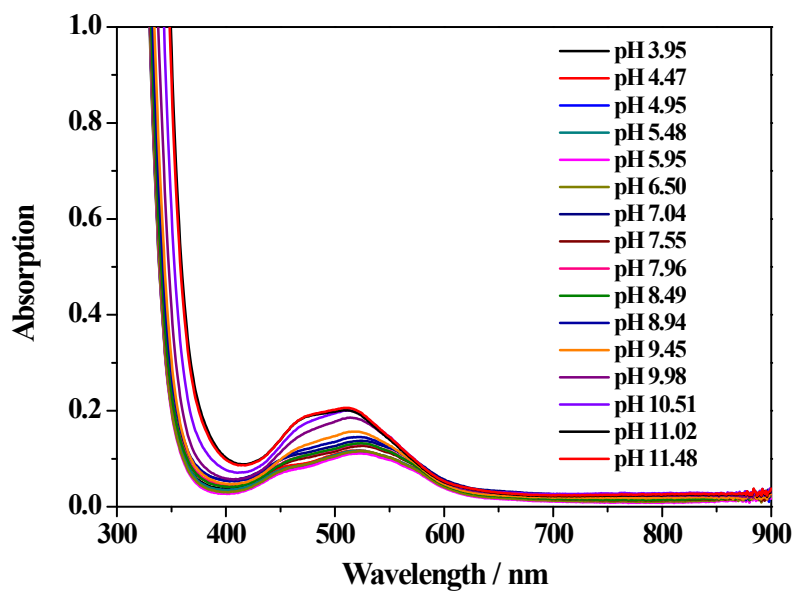


Fig. S7 pH dependent UV-vis spectra of 5 mM of complex 1 in 0.1 M PBS.

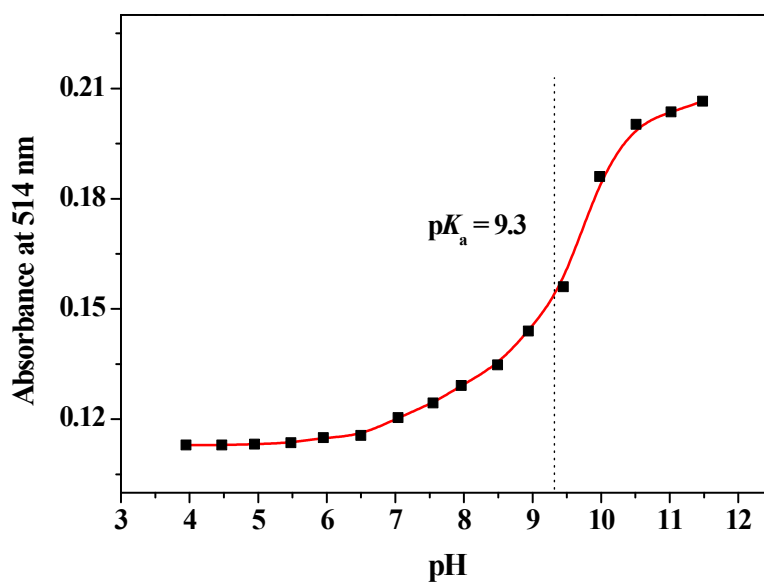


Fig. S8 Representative plot of the absorbance at 514 nm of complex 1 vs. pH value of 0.1 M PBS.

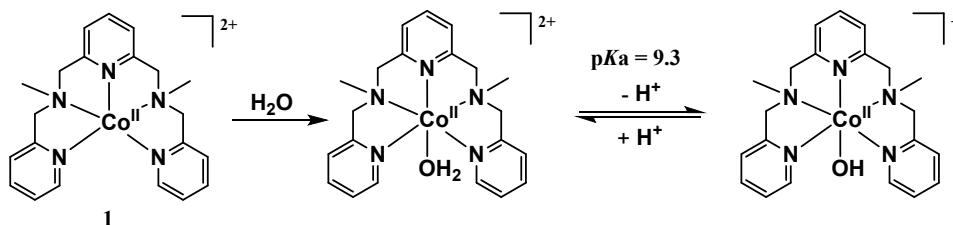


Fig. S9 Protonation-deprotonation equilibrium of complex 1 in 0.1 M PBS.

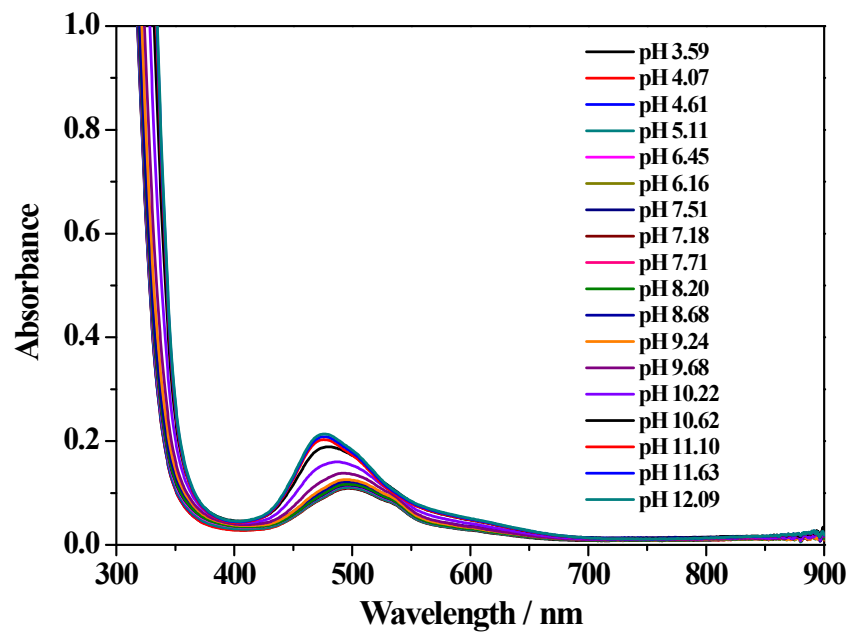


Fig. S10 pH dependent UV-vis spectra of 5 mM of complex **2** in 0.1 M PBS.

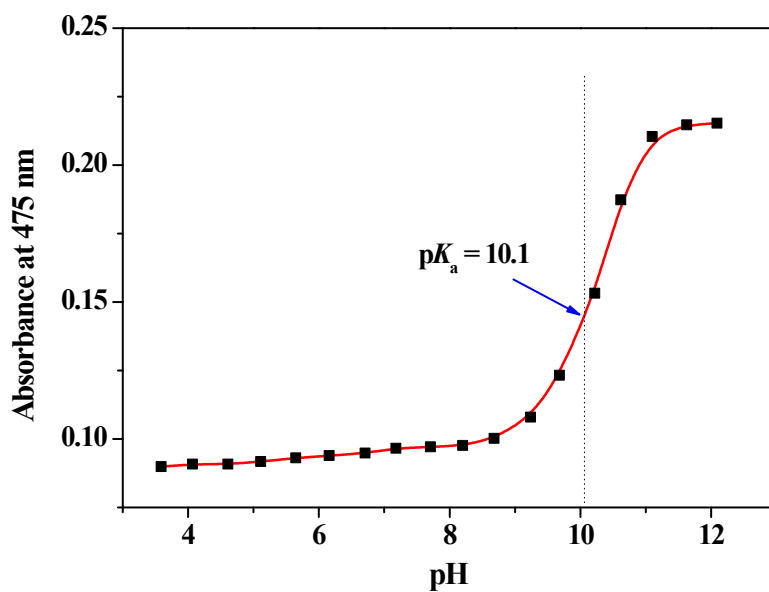


Fig. S11 Representative plot of the absorbance at 475 nm of complex **2** vs. pH value of 0.1 M PBS.

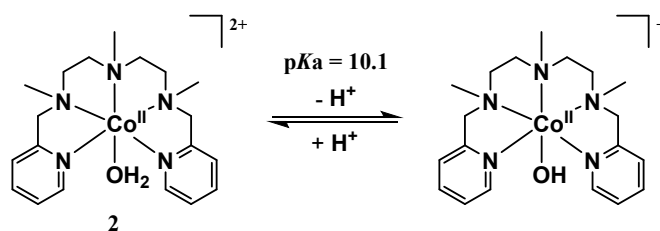


Fig. S12 Protonation–deprotonation equilibrium of complex **2** in 0.1 M PBS.

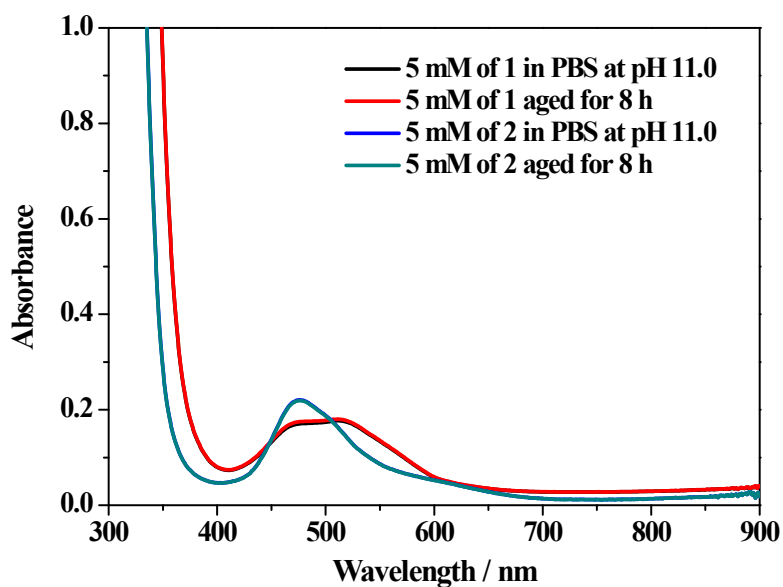


Fig. S13 UV-vis absorption spectra of 5 mM of complex **1** and **2** in 0.1 M PBS at pH 11.0 before and after 8 hours aging time.

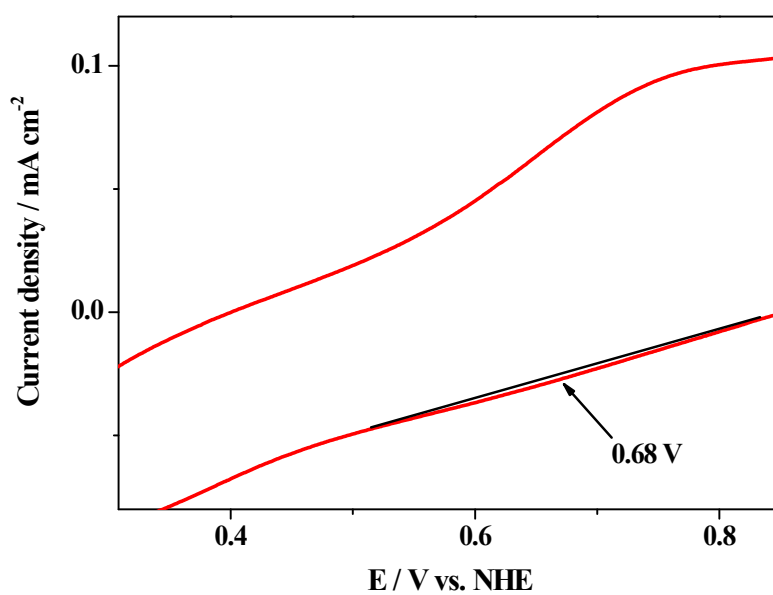


Fig. S14 CV curves of 1 mM of complexes **1** in 0.1 M PBS at pH 11.0, GC electrode as working electrode, scan rate = 100 mV/s.

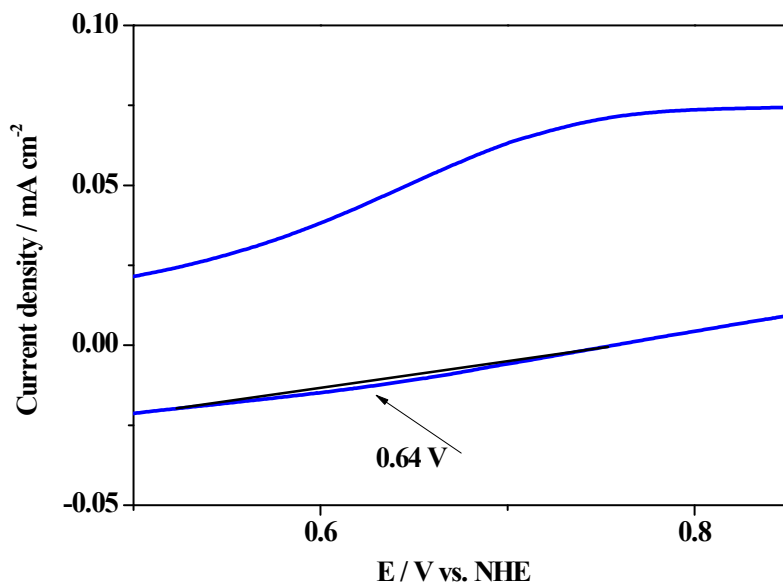


Fig. S15 CV curves of 1 mM of complexes **2** in 0.1 M PBS at pH 11.0, GC electrode as working electrode, scan rate = 100 mV/s.

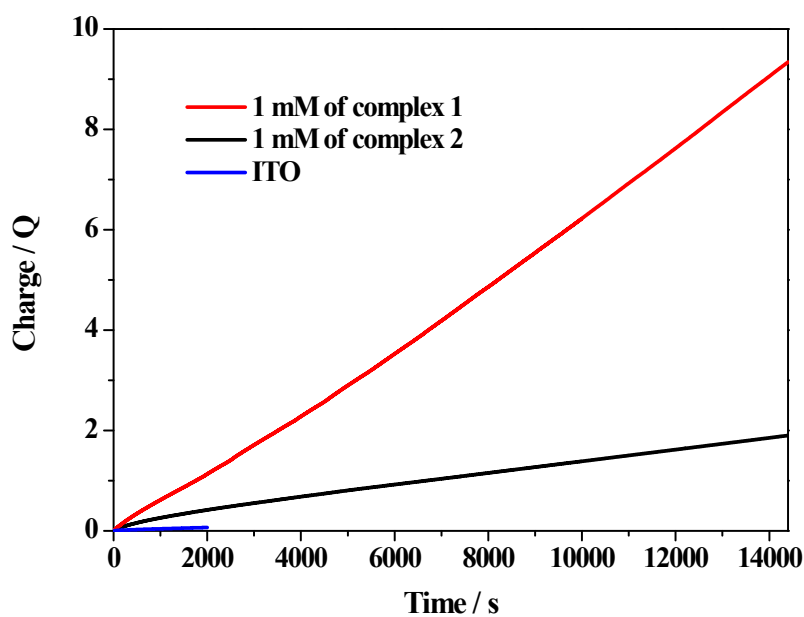


Fig. S16 Chronocoulometric ($Q = \text{charge vs. time}$) plot from controlled potential electrolysis with 1 mM of **1** or 1 mM of **2** at ITO working electrode and pH 11.0 (0.1 M PBS) at an applied potential of 1.55 V vs. NHE. A charge-versus-time trace for the background ITO electrode is also shown.

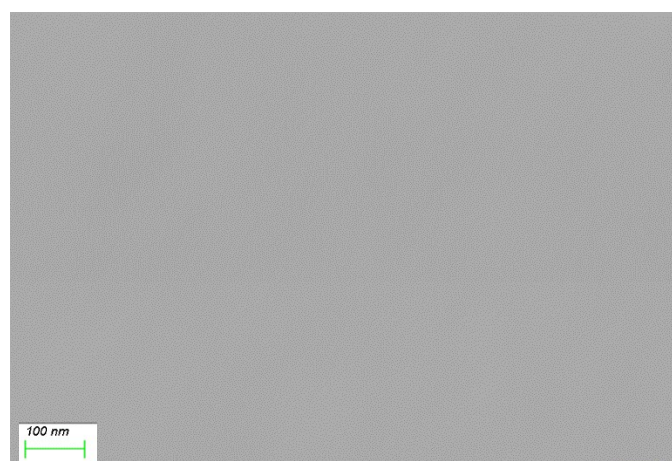
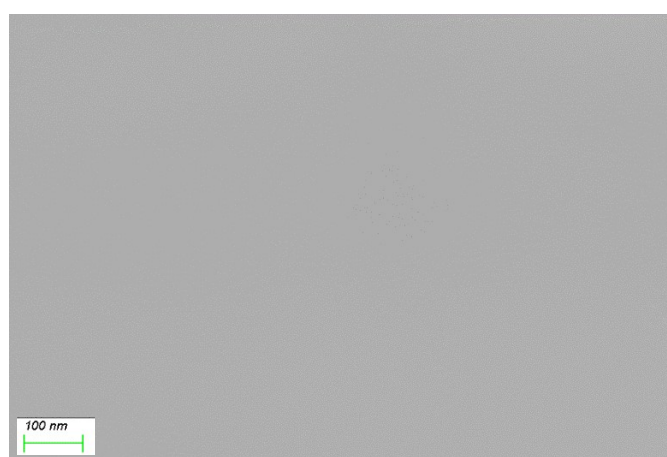
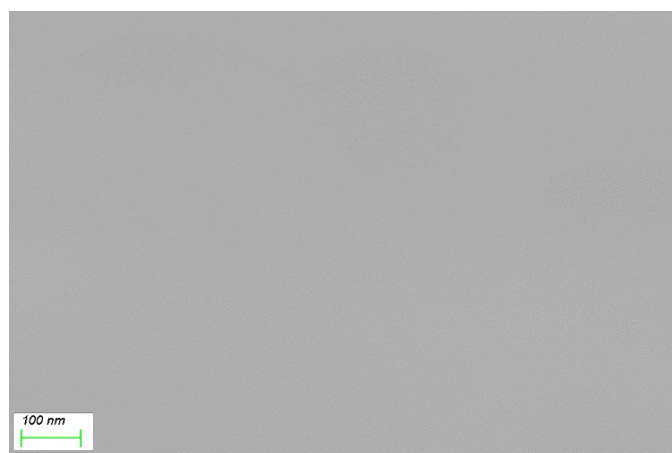


Fig. S17 SEM images of the surface of ITO electrode before (top) and after 4 h CPE experiments of 1 mM of **1** (middle) and 1 mM of **2** (bottom) in 0.1 M PBS at pH 11.0.

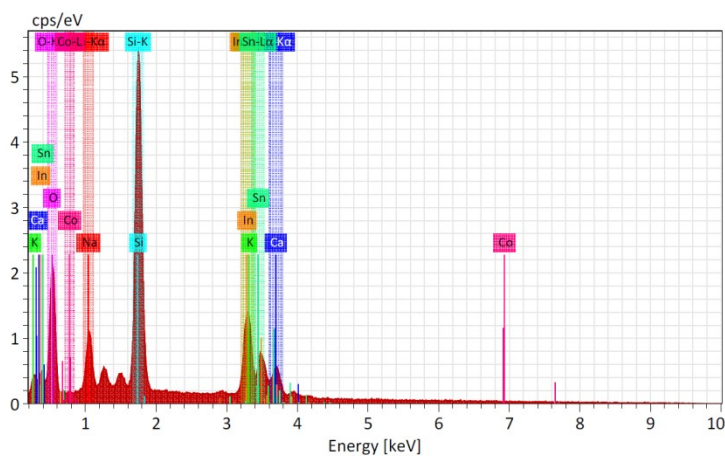
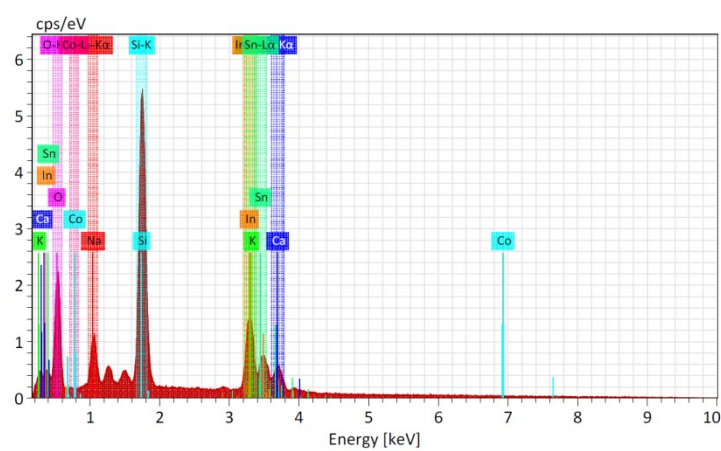
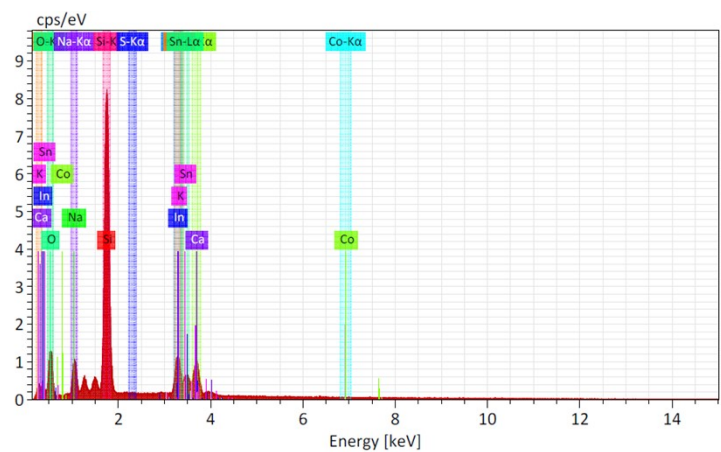


Fig. S18 EDX analysis of the surface of ITO electrode before (top) and after 4 h CPE experiments of 1 mM of **1** (middle) and 1 mM of **2** (bottom) in 0.1 M PBS at pH 11.0.

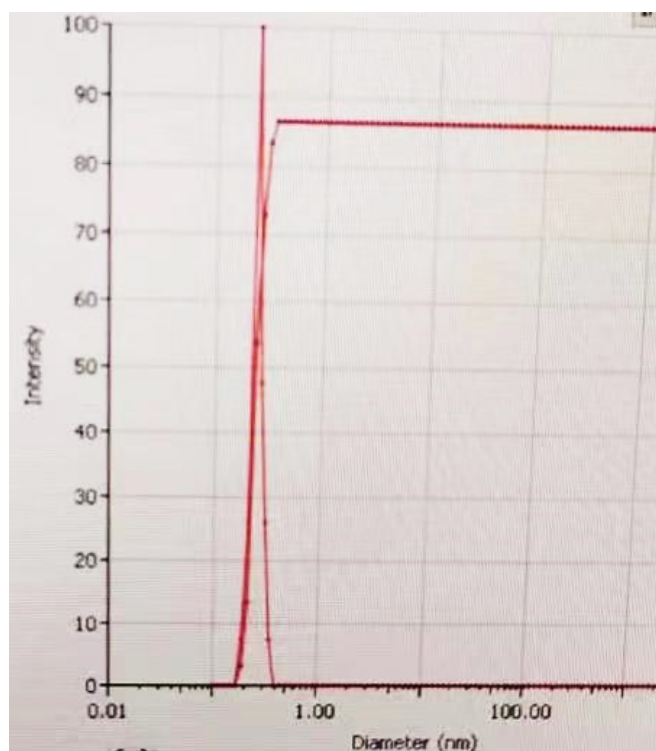


Fig. S19 Dynamic light scattering (DLS) measurement of the electrolyte solutions after 4 h CPE experiment of complex **1**. The signal at diameter below 1 nm is ascribed to the background signal of true solution.¹

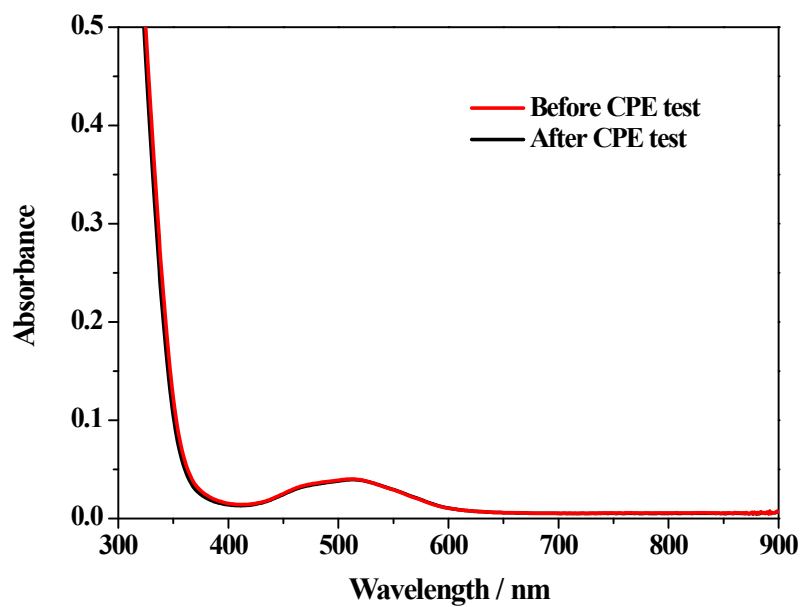


Fig. S20 UV-vis absorbance spectra of 1 mM of complex **1** before and after 4 h CPE test at 1.55 V vs. NHE, 0.1 M PBS at pH 11.0 was used as electrolyte.

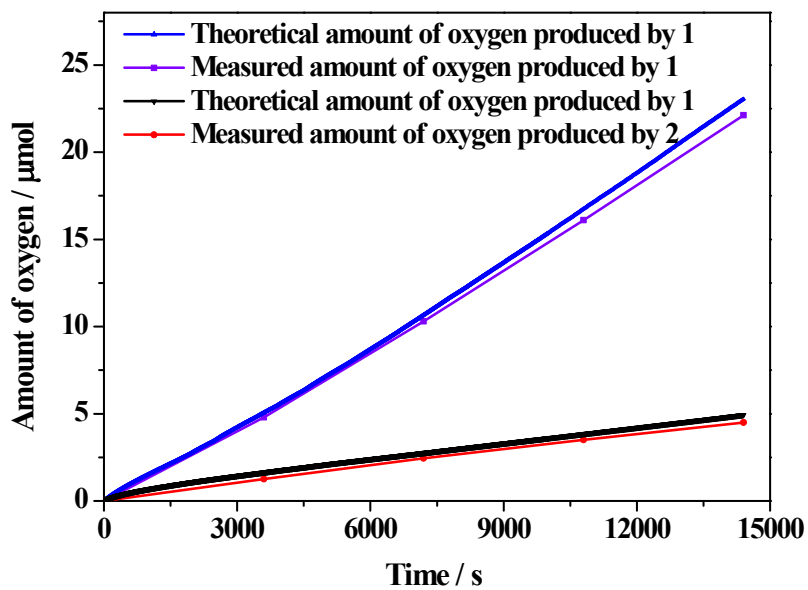


Fig. S21 Faradaic efficiency of O_2 evolution for complex **1** and complex **2** under electrolysis of 14400 s at 1.55 V (vs. NHE) in 0.1 M PBS at pH 11.0.

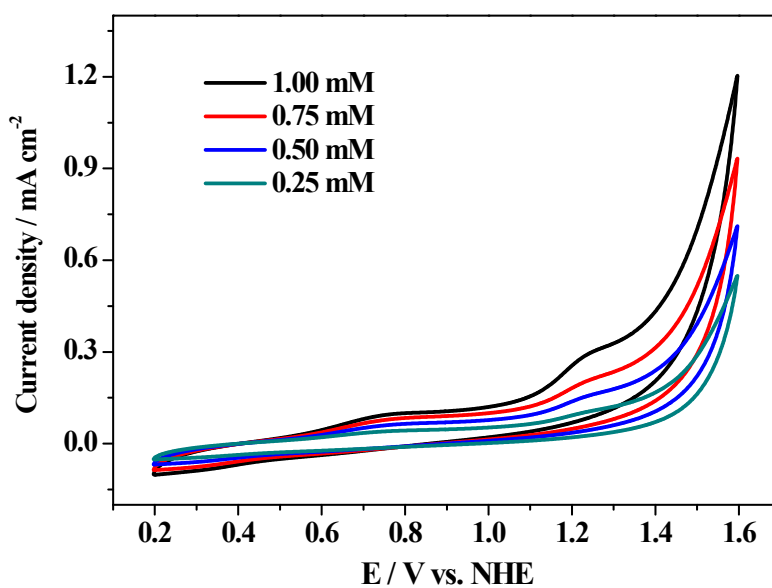


Fig. S22 CV of complex **1** with various concentrations in 0.1 M PBS at pH 11.0.

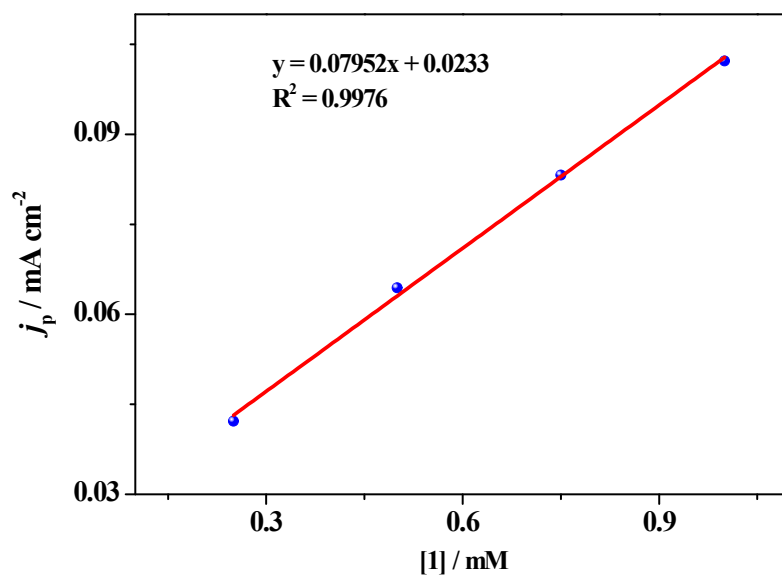


Fig. S23 Relationship between current of anodic wave and concentration of complex **1**, scan rate = 100 mV/s, 0.1 M PBS at pH 11.0 as electrolyte.

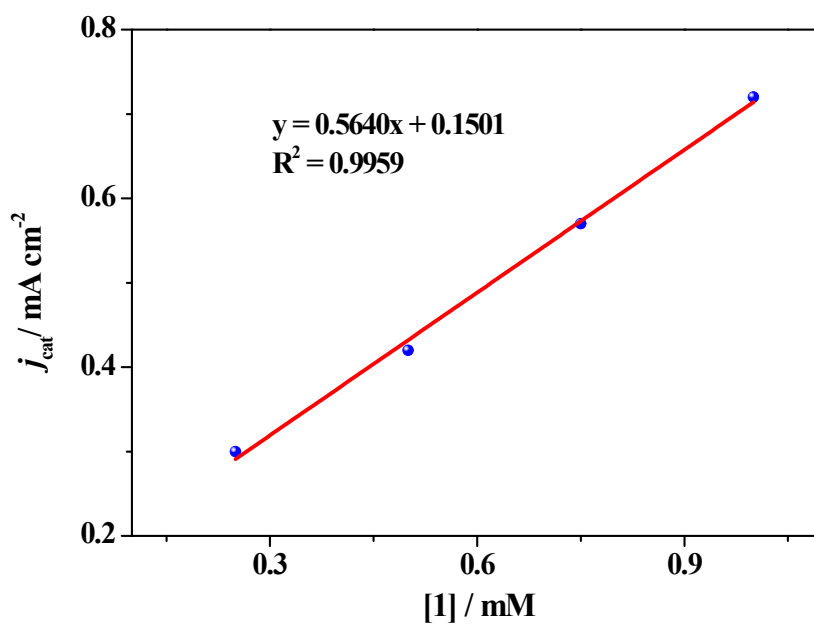


Fig. S24 Relationship between current density at 1.55 V vs. NHE and concentration of complex **1**, scan rate = 100 mV/s, 0.1 M PBS at pH 11.0 as electrolyte.

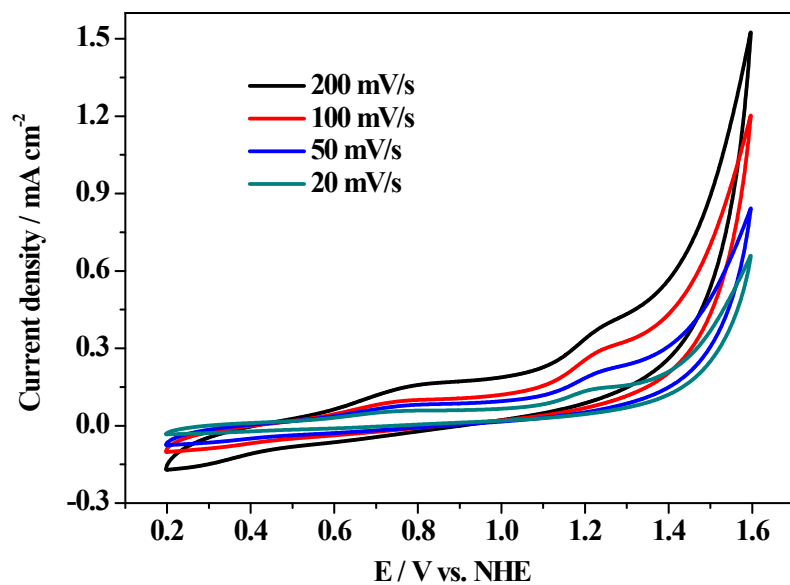


Fig. S25 CV of 1.0 mM of **1** with various scan rates, 0.1 M PBS at pH 11.0 as electrolyte.

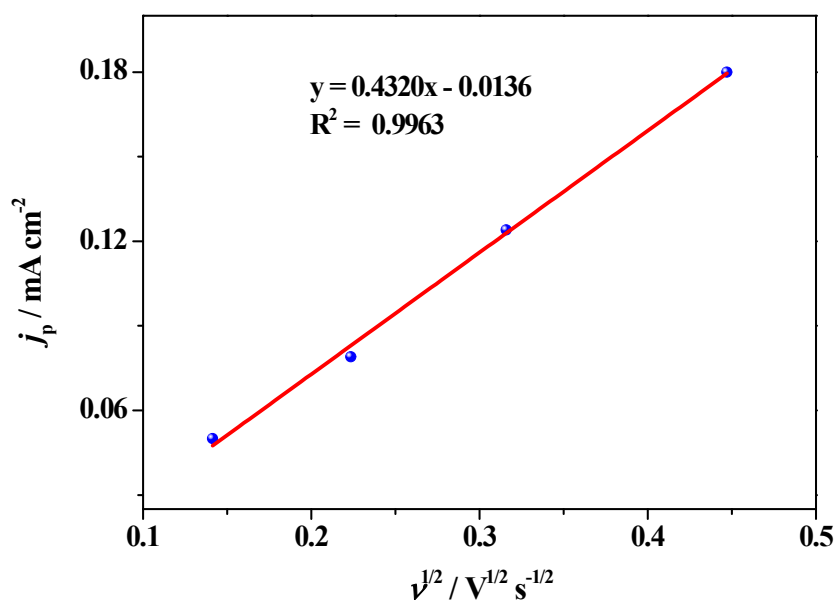


Fig. S26 Dependence of oxidation wave current density of the non-catalytic process of 1 mM of **1** on the square root of scan rates, 0.1 M PBS at pH 11.0 as electrolyte.

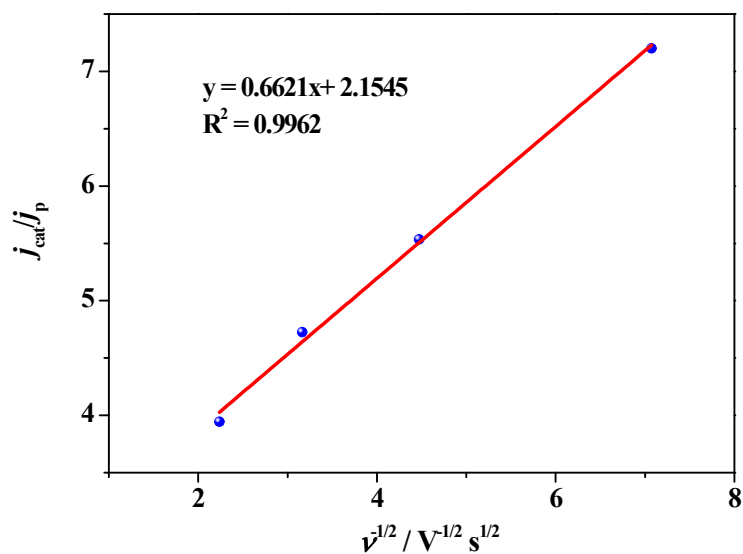


Fig. S27 Plots of the ratio of j_{cat} to j_p of complex **1** versus the reciprocal of the square root of scan rate.

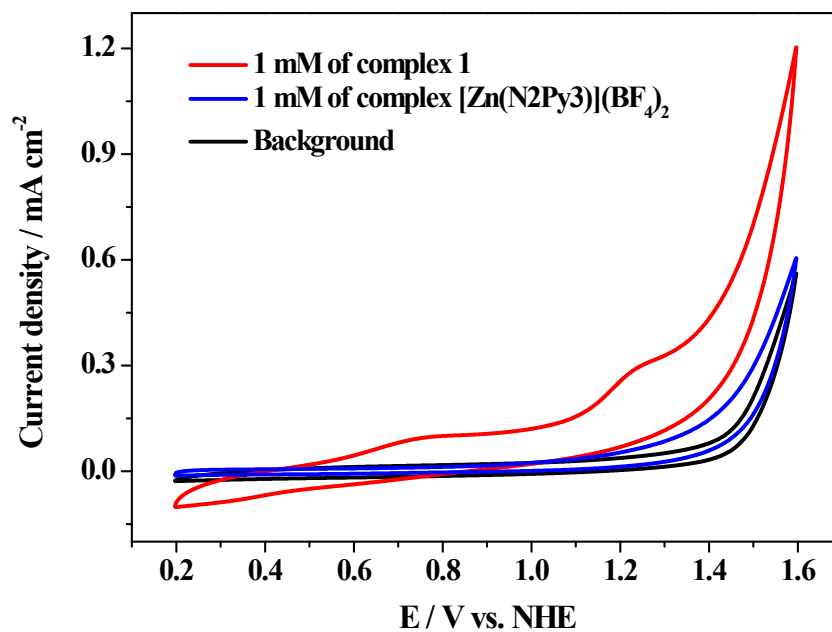


Fig. 28 CV curves of 1 mM of complexes **1** and $[Zn(N2Py3)](BF_4)_2$ in 0.1 M PBS at pH 11.0, GC electrode as working electrode, scan rate = 100 mV/s.

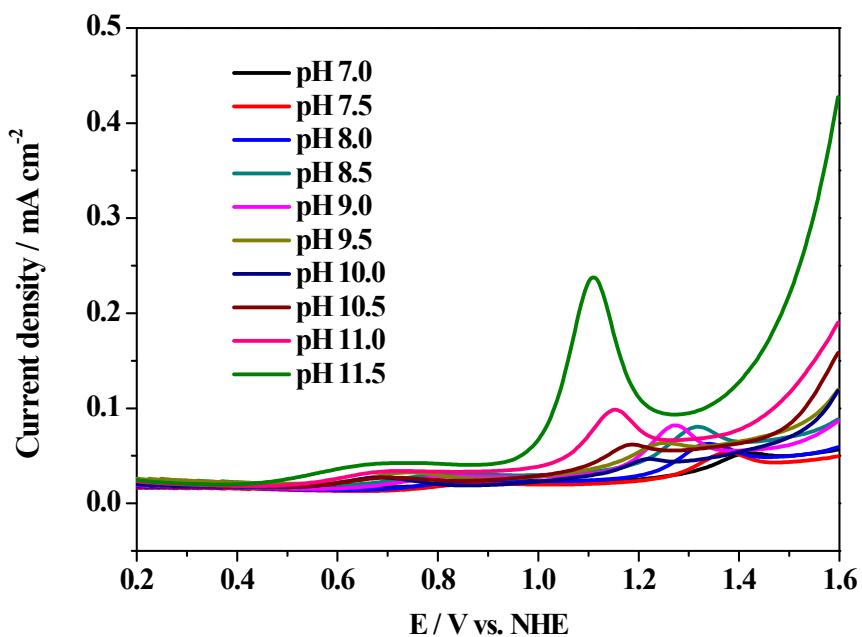


Fig. S29 Differential pulse voltammetry (DPV) examination of 1 mM complex **1** in 0.1 M PBS at various pH values.

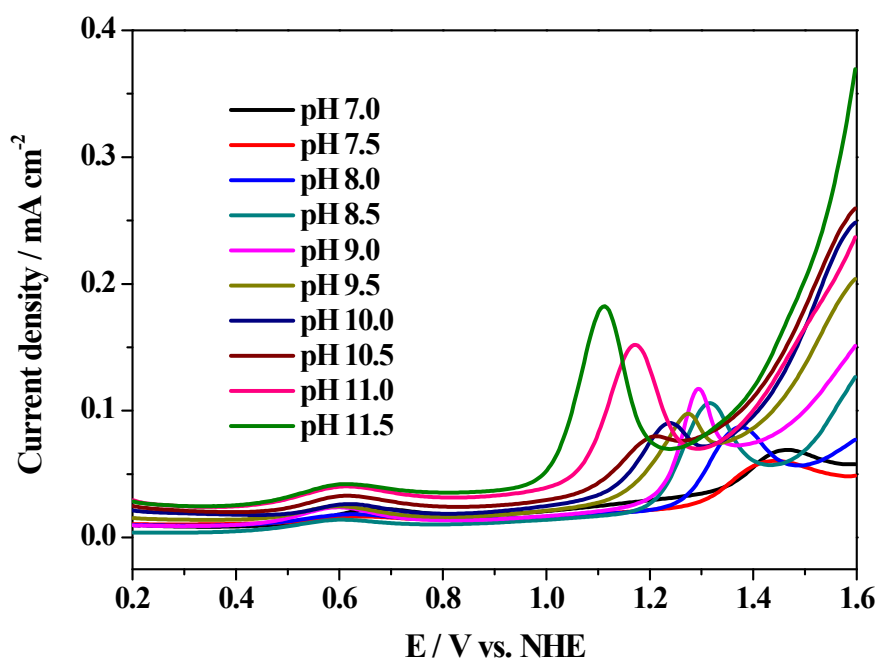


Fig. S30 Differential pulse voltammetry (DPV) examination of 1 mM complex **2** in 0.1 M PBS at various pH values.

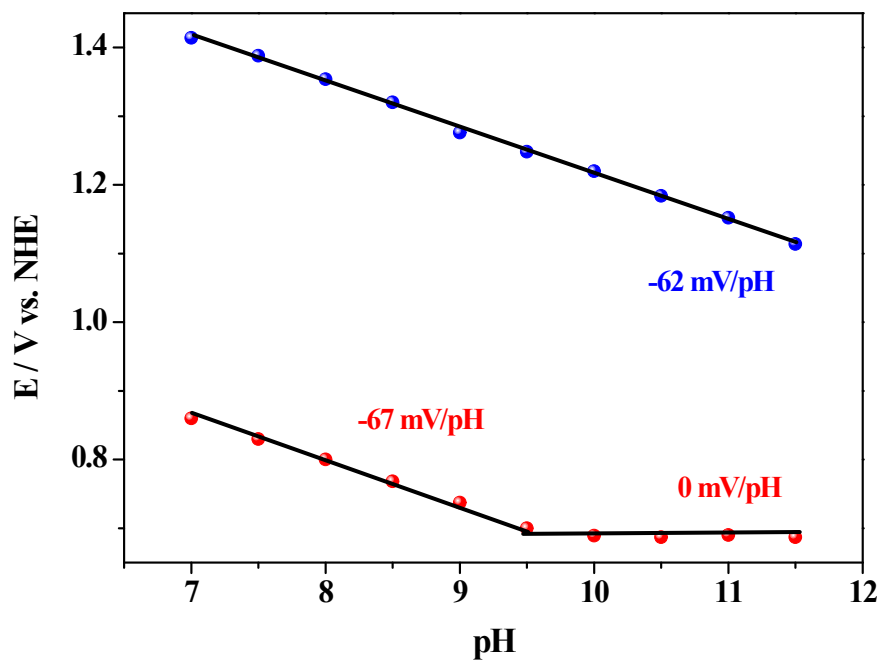


Fig. S31 The relationship between the potential of each redox couple of complex 1 and the pH value of electrolyte.

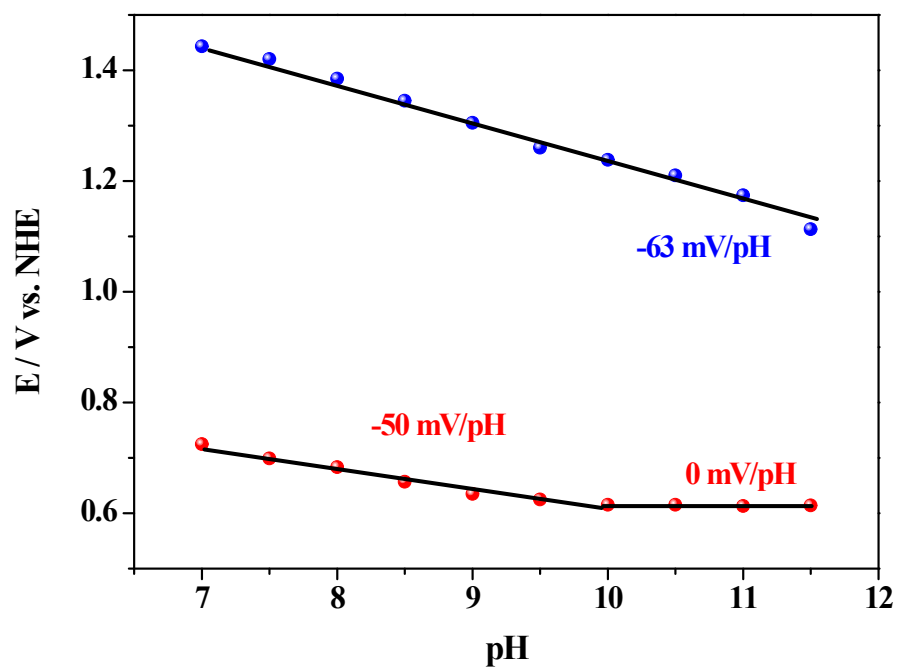


Fig. S32 The relationship between the potential of each redox couple of complex 2 and the pH value of electrolyte.

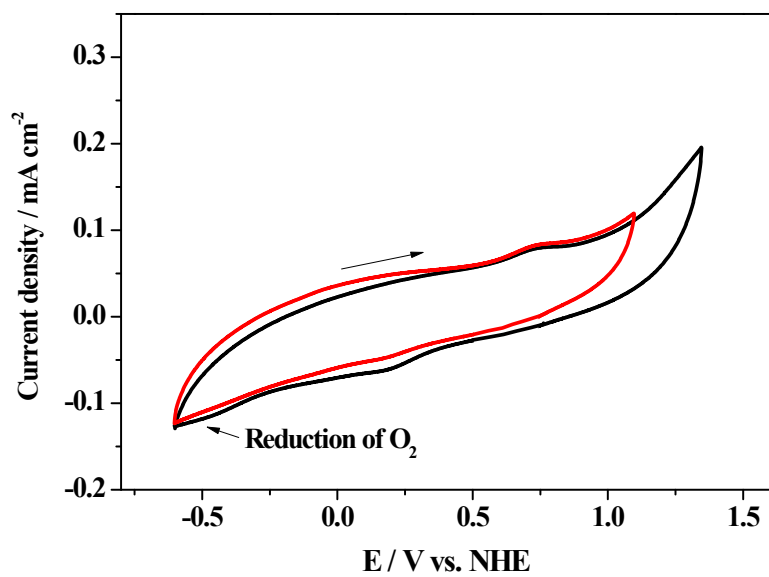


Fig. S33 The reduction process of oxygen production by ligand-assistant water oxidation catalyzed by complex **1**.

Reference

- S1 L. Wang, L. Duan, R. B. Ambre, Q. Daniel, H. Chen, J. Sun. B. Das, A. Thapper, J. Uhlig, P. Dinér and L. Sun, *J. Catal.*, 2016, **335**, 72–78.